Journal of Engineering and Technology for Industrial Applications

ITEGAM-JETIA

Manaus, v.12 n.58, p.1205-1214. March/April, 2026.
DOI: https://doi.org/10.5935/jetia.v12i58.3291

ISSN ONLINE: 2447-0228

RESEARCH ARTICLE OPEN ACCESS

ENHANCING BIODIESEL YIELD FROM CANOLA OIL THROUGH RESPONSE SURFACE METHODOLOGY: IN-DEPTH STUDY OF REACTION PARAMETERS AND ENGINE EFFICIENCY

Sangeetha Krishnamoorthi*[1], Prabhu L[2], Saravanan M[3], Mahesh R[4], Hariharan R[5], Venu Kumar B R[6]

[1, 2, 3,4,5,6]Department of Mechanical Engineering, Aarupadai Veedu Institute of Technology, Vinayaka Mission's Research Foundation (DU), Tamil Nadu, India.

[1]https://orcid.org/0000-0003-1427-8743, [2]https://orcid.org/0000-0001-9019-4555, [3]https://orcid.org/0000-0002-6717-3315, [4]https://orcid.org/0000-0002-3438-8715, [5]https://orcid.org/0009-0005-5329-4705, [6]https://orcid.org/0009-0000-5075-6832

Email: *geetha30981@gmail.com

ARTICLE INFO

Article History
Received: January 12, 2026
Reviewed: February 14, 2026
Accepted: March 26, 2026
Published: April 30, 2026

Keywords:
Response surface methodology,
Efficiency,
Specific fuel consumption,
ANSYS,
Biodiesel production ,
Exhaust emissions,
Stoichiometric Ratio.

ABSTRACT

The response surface methodology (RSM) was employed to ascertain the most favorable operating conditions for the transesterification process of canola oil. These conditions encompassed the stoichiometric ethanol-to-oil ratio, reaction temperature, and reaction duration, all of which contributed to the maximization of biodiesel output. With an R2 value of 91.43%, the RSM model was statistically significant. Fourier transform infrared spectroscopy (FTIR) and gas chromatography (GC)-mass spectrometry confirmed that the majority of triglycerides were formed as methyl ester. When compared to pure petro-diesel and biodiesel blends, the performance and emissions of the biodiesel produced were found to be promising in a diesel engine.

I. INTRODUCTION

A global solution to the ever-increasing demand for energy is urgently required. Sulfur dioxide, carbon dioxide, particulate matter, and other gas emissions from burning fossil fuels are a major source of pollution, and these resources are finite [1]. The renewable alternative biodiesel, made from canola oil, is becoming more popular for use in diesel engines. Vegetable oils used for frying produce copious amounts of Canola Oil, which face disposal challenges. The production of biodiesel using them has the advantage of being both cost-effective and environmentally conscious [2]. Transesterification, the prevailing method employed in biodiesel production, entails catalysed chemical reactions between alcohol and vegetable oil [3], [4]. The majority of the biodiesel production budget goes into buying the essential raw materials. Biodiesel production is able to maintain its low cost by utilising inexpensive raw materials that comprise fatty acids.

Things like animal fats, and vegetable oil by-products fall under this category. The most popular and least expensive raw material for biodiesel production is CO, followed by palm oil, jatropha oil, and soy bean oil [5], [6]. Particulate matter, unburned hydrocarbons, and carbon monoxide are all reduced when biodiesel is burned compared to petrodiesel fuel. Reduced emissions of sulphur dioxide are a side effect of burning biodiesel, which is derived from natural sources and hence contains less sulphur [7], [8]. Various scholars have put forward mathematical models that aim to optimise the circumstances for transesterification. The authors [9] utilized ANN and RSM as mathematical models to predict the biodiesel yield. The authors [10] ,[11] ANN model was used to manufacture biodiesel from used cooking oil [12].

This study aimed to maximize the biodiesel yield from COs by studying the main factors of the transesterification reaction using the RSM approach. It highlighted the process's benefits, shortcomings, and optimal circumstances. A comparison was made between the biodiesel's properties and the European standard. The quality of biodiesel generated from CO was assessed and investigated its effects on engine performance. We looked at the proposed flow sheet and the features of the engine exhaust pollutants.

II. MATERIALS AND METHODS

A combination of canola oil, potassium hydroxide, phenolphthalein, distilled water, high-purity sodium hydroxide, ethanol, and canola oil were used in this experiment.

II.1 FEEDSTOCK PRETREATMENT

CO needs to be disposed of because it includes certain contaminants.

1) The oil is first filtered by screening it to eliminate any solid particles.
2) The leftover solids in the oil are settled after 24 hours of filtering by letting it settle in the tank.
3) To get rid of any remaining debris or particles in the oil, a second filtering process is employed.
4) For 30 minutes, the oil is heated to 80°C in order to evaporate any moisture.

II.2 BIODIESEL PRODUCTION

The transesterification reaction was used to produce biodiesel. This was carried out in a 500 mL conical flask with 300 g of CO in a laboratory-scale batch method. The experimental design dictated that the alcohol ratio be adjusted in relation to the time (t), temperature (T), and stoichiometric ratio (S) for each run [13], [14]. The proportion of NaOH supplied to each sample was determined by its free fatty acid (FFA) content, and all of the samples were mixed using a magnetic stirrer set to 250 rpm.

II.2.1 FABRICATION OF ETHANOL CATALYST SOLUTION

The proportion of FFA was used to alter the ethanol to NaOH ratio: One weight % oil was used as a catalyst when the free fatty acid concentration was less than 1%; when the free fatty acid concentration was greater than 1%, the catalyst was [% FFA] 0.144 plus 1% [15].

II.2.2 REACTION CONDITIONS

A mechanical stirrer was used to mix the oil with the ethanol catalyst solution at 250 rpm until the reaction was complete, after the necessary temperature had been set. The variables that were examined included time, stoichiometric ratio, and temperature [16], [17]. Table. 1 shows the ranges of these variables.

II.2.3 TRANSESTERIFICATION REACTION RESULTS ANALYZED STATISTICALLY

The experimental Statistical Design-Expert 11.1.2 Box-Behnken approach was implemented in order to optimise the transesterification process. To determine the quantity of runs, employ the subsequent formula [18], [19]:

$$N=2k(k-1)+ C_0 \quad (1)$$

C_0 constant no of trails at average conditions
N no of trails
k no of variables.

The mixture was funneled to separate the reactants once the reaction was finished and then permitted to sit for 24 hours. Because of this, the crude ester phase and the glycerol phase were able to separate. Table. 1 displays the values selected for every factors.

Table 1: Experimented parameters.

Factors	Minimum.	Midpoint	Maximum
Time (t)	40	60	80
Stochiometric Ratio (S)	1:4	1:6	1:8
Temperature (T)	30	60	90

Source: Authors, (2026).

While the glycerol was emptied from the bottom of the separating funnel, the container containing the biodiesel crude ester remained unchanged. Following this, the crude ester (biodiesel) underwent two washes using heated water containing 50 vol % biodiesel at 60°C until the formation of two distinct layers became apparent [20], [21]. At eliminate any remaining moisture, the biodiesel was dried in a drier set to 110°C for a duration of thirty minutes.

III. RESULTS AND DISCUSSIONS

Table 2 displays the outcome of the statistical analysis. Time (t), temperature (T), and stoichiometric ratio (S) are the three variables under investigation, and their interplay can be investigated using statistical design analysis.

Table 2: Design of experiments.

Run	t [min]	T [°C]	S	Conv. [wt %]
1	60	60	6	96.79
2	60	60	6	97.07
3	40	60	4	87.99
4	60	30	4	85.25
5	60	90	4	89.19
6	40	30	6	98.17
7	80	90	6	92.42
8	60	60	6	97.4
9	60	60	6	97.89
10	60	90	8	94.17
11	60	60	6	97.22
12	80	60	4	87.47
13	80	30	6	99.65
14	80	30	8	96.3
15	60	30	8	96.1
16	40	90	6	94.07
17	40	60	8	99.32

Source: Authors, (2026).

In order to ascertain the impact of altering the S on the biodiesel yield, the researchers calculated t and T while subjecting it to its minimal, maximal, and mean values. A larger yield was also achieved by increasing the stoichiometric ratio, particularly when the reaction was allowed to run for the maximum period of time at a low temperature of 30°C (80 min). The effects of temperature T on reaction time t and stoichiometric ratio S variables were studied across a range of lowest, maximum, and average values to assess biodiesel synthesis. At the maximum S of alcohol to oil (8:1) and within the designated reaction period, the yield can be enhanced by lessening the T to either its minimal of 30°C or its mean of 60°C. The inverse proportionality remains unaffected by temperature variations (80 min). The two variables, along with the S and T, demonstrated a direct proportional relationship with the biodiesel production, according to an examination of the effects of altering t to its minimal, maximal, and mean values.

An approach to augmenting the yield involves extending the duration of the reaction. The best yield is achieved with an 80-minute t, a feed T of 30°C, and a high S of 8:1 alcohol to oil. To plot every testing outcome, a 3D cube is utilized (Figure 1). With every point situated on its periphery, the Box-Behnken pattern is unmistakably spherical. In the Box-Behnken design, each variable's upper and lower limits define a cubic zone where no points are situated at its corners. The reaction yield-determining three parameters are shown along the X-axis by the minimum value of t, the Y-axis by the maximum value of T, and the Z-axis by the maximum value of the S between the alcohol and oil T. According to the cubic model, the optimal conditions for achieving a maximum yield of 98.22% include an 80-minute t, an 8:1 S, and a minimum T of 30°C.

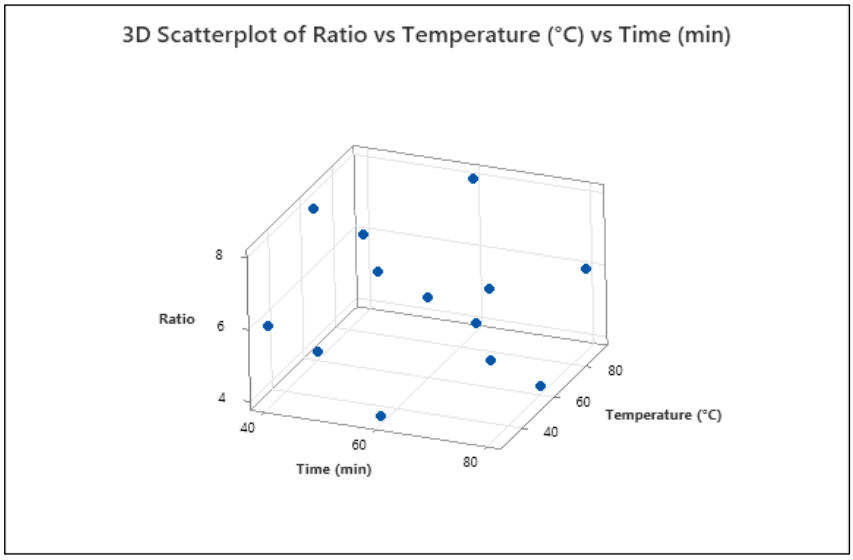

Figure 1: 3D graph depicting the outcomes of canola oil biodiesel production.
Source: Authors, (2026).

The minimal yield achieved was 82.15 %, as seen in the top right forward-facing edge of the cubic model. This was accomplished at a T of 90°C, a t of 80 minutes, and a low S of 4:1. The projected cubic model possesses a statistically significant R2 value of 91.43 % and a P-value below 0.0001. Utilizing a S of 8:1, a maximum biodiesel recovery of 98.22% was achieved in 80 min at 30°C during the reaction. In order to validate the results, five runs were conducted under the parameters previously indicated. The findings indicated that the average recovery of biodiesel was 95.66 %, with a standard deviation of 1.974 %. Since the margin of error did not go beyond 2.6%, this demonstrates that the proposed model is valid.

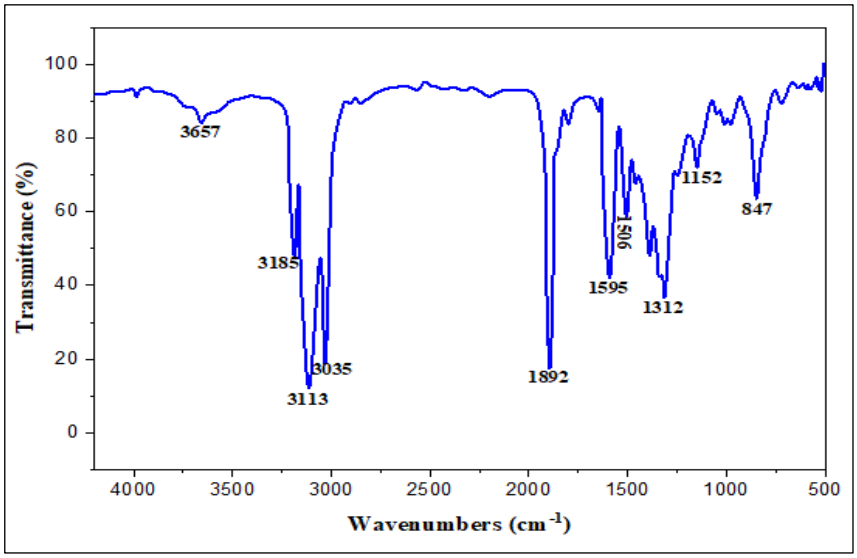

Figure 2: FTIR analysis.
Source: Authors, (2026).

As demonstrated in Figure 2, the CO biodiesel sample was compared to a standard sample and described using FTIR. The existence of the following biodiesel properties peaks was observed in the first sample, as shown in Fig 2. There were stretching absorption peaks at 3657, 3185, and 1892 cm^{-1} for OH, =CH, and C=O, respectively. There were two maxima for the stretching vibrations of the -CH2 groups: one at 3113 cm^{-1} and the other at 3035cm^{-1} . The C-O-C stretching vibration absorption maxima at 1152 and 1312cm^{-1} were determined to be anti-symmetric and symmetric, respectively, according to reference [22], [23]. In Table 3, you can see the biodiesel characterization results.

Table 3: Specification of results.

Properties	Units	Optimal sample	European biodiesel standard
Flash point	[C]	92	> 90
Calorific value	[MJ kg^{-1}]	40.49	38.31
Density at 15 C	[kg m^{-3}]	882.5	870–900
Acid range	[mg KOH/g]	0.133	0.6
Viscosity at 40°C	[mm^2s^{-1}]	4.40	3.6–5.2
Sulfur	[mg kg^{-1}]	0.004	10

Source: Authors, (2026).

The study employed a TG WAX-MS direct capillary column equipped with a 0.3 mm ± 0.25 mm film thickness and a gas chromatography to determine the biodiesel sample's chemical arrangement. Following three minutes of holding at 90°C, the oven was progressively heated to 300°C for 24 minutes at a rate of 15°C per minute. The data confirming the synthesis of methyl ester from the majority of triglycerides, which is pertinent to biodiesel, are presented in Table 4.

Table 4: Gas Chromatography analysis for the arranged biodiesel.

Time [min]	Compound	Area Pct
12.45	$C_{15}H_{30}O_2$	0.67
13.95	$C_{17}H_{34}O_2$	21.80
14.96	C19H34O	43.61
15.49	$C_{19}H_{36}O_2$	9.63
16.07	$C_{21}H_{40}O_2$	4.24
16.18	$C_{21}H_{42}O$	3.40
16.56	$C_{15}H_{20}O_5$	2.71
16.92	$C_{15}H_{26}O$	2.03
17.17	$C_{23}H_{46}O$	2.85
17.64	$C_{24}H_{48}O_2$	0.62
18.11	$C_{25}H_{50}O_2$	4.31
18.56	$C_{30}H$	0.84
18.99	$C_{27}H_{54}O_2$	1.72

Source: Authors, (2026).

This study examines the efficiency and pollution levels of a diesel, CO biodiesel, and blended biodiesel engine that is single-cylinder, four-stroke, air-cooled, and direct-injection (B25, B50, and B75, where B25, e.g., means 25 % biodiesel Performance and emission parameter results are founded upon research conducted on several factors including air-fuel ratio (AFR), volumetric efficiency (VE), exhaust gas temperature (EGT), thermal efficiency (TE), specific fuel consumption (SFC), and concentrations of HC, CO, O2 and CO2 emissions [24], [25].

The average value after running each run three times we recorded. Less than 0.25 was the standard deviation. Figure 3 shows the specific fuel consumption of biodiesel, mixed biodiesel, and Petro diesel in relation to the brake power of engine. As the engine load increases, it falls. Samples of biodiesel and Petro diesel had the greatest and lowest specific fuel consumption values, respectively. Typically, as the percentage of biodiesel increases, the particular fuel consumption also rises. The reason for this is because biodiesel and its mixes have a higher viscosity and a lower heating value than Petro diesel. When operating at full load, the specific fuel consumption values for B100, B75, B50, B25, and D100 were 0.59, 0.66, 0.59, 0.58, and 0.49, respectively [26].

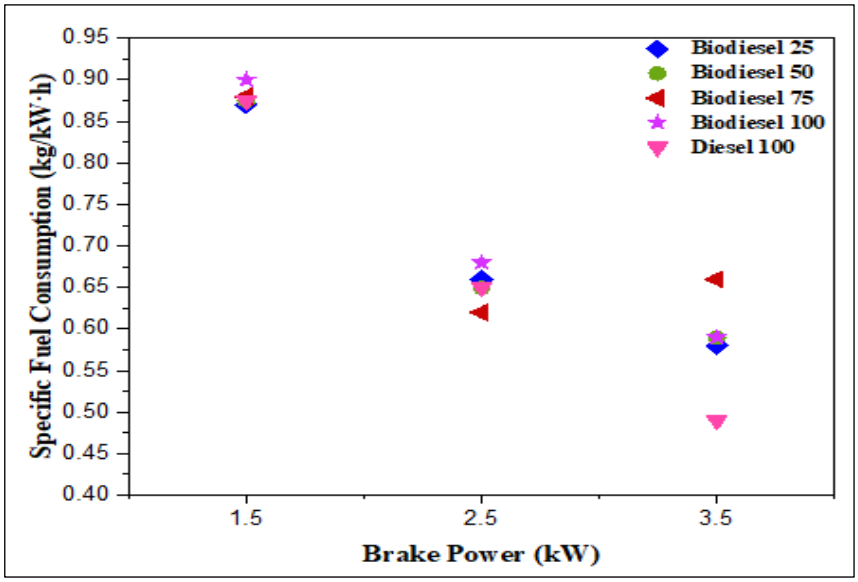

Figure 3: Comparison of SFC with engine load for various composition of diesel.
Source: Authors, (2026).

Figure 4 shows the relationship between the engine's braking power and the thermal efficiency of biodiesel, mixed biodiesel, and petrodiesel samples. For all fuels, it rises as engine load increases. Increasing the amount of petrodiesel in each sample improves thermal efficiency because biodiesel has a lower calorific value than petrodiesel and its ignition delay is smaller, causing combustion to begin before the top dead centre. Because of this, the engine's thermal efficiency drops because compression work and heat loss are both increased. Maximum load operation yielded thermal efficiency values of 22.2 % for B100, 16.66 % for B75, 20.39 % for B50, 22.42 % for D100, and 24.64 % for B25 [27].

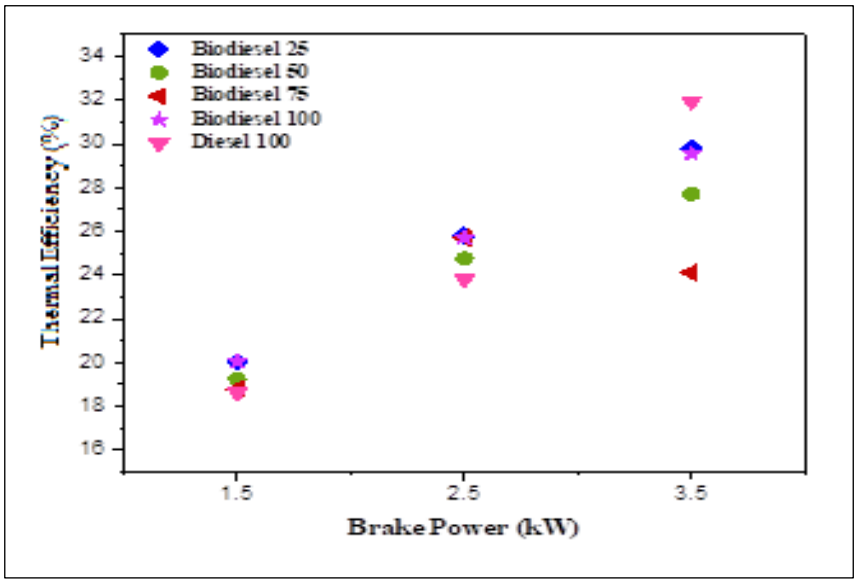

Figure 4: Comparison of thermal efficacy with engine load for various composition of diesel.
Source: Authors, (2026).

Figure 5 shows the temperatures of the exhaust gases as a function of the engine's braking power for three different types of biodiesel samples: petrodiesel, mixed biodiesel, and biodiesel. The temperature of the exhaust gas will increase for every sample as the engine load increases. Typically, the temperature of the exhaust gas increases as the percentage of petrodiesel in each sample increases. On full load, the exhaust gas temperatures for B100, B75, B50, B25, and D100 were 262.90, 291.22, 346.91, 279.07, and 338.89°C, respectively [28].

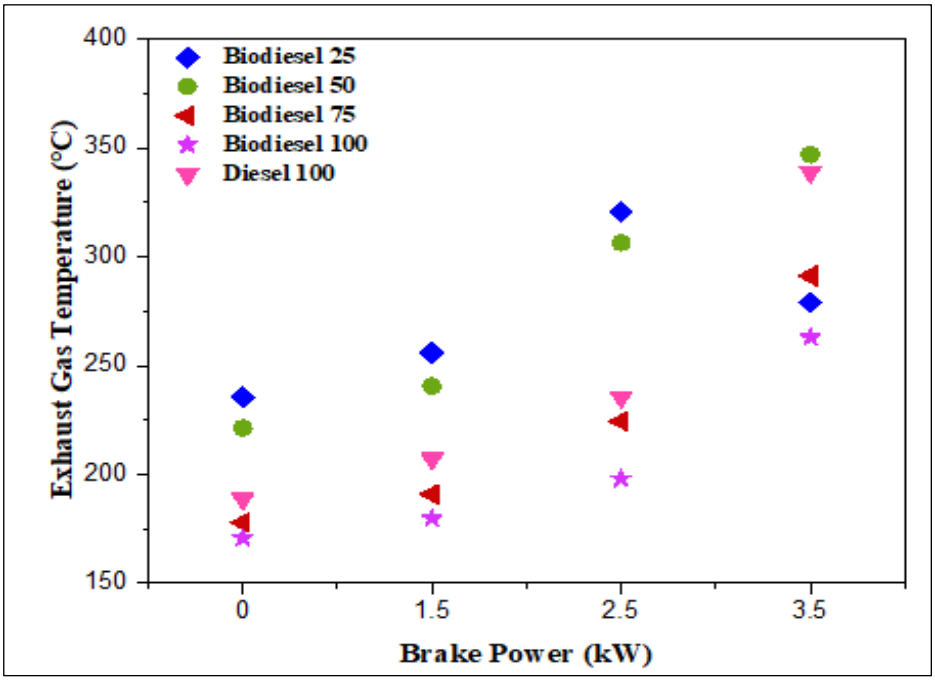

Figure 5: Comparison of EGT with engine load for various composition of diesel.
Source: Authors, (2026).

Figure 6 illustrates the effect of volumetric efficiency on the braking force of the engine. Samples of biodiesel, mixed biodiesel, and petro-diesel were utilised to evaluate the engine. While biodiesel, blended biodiesel, and petrodiesel all had good volumetric efficiencies at low engine loads, the retained exhaust gases' higher temperatures caused the efficiencies to drop at high engine loads. By warming and reducing the density of the incoming fresh air, the retained exhaust gases enhance both the volumetric efficiency and the reduction in the amount of air required to supply the combustion chamber. At maximum load operation, the volumetric efficiency values for B100, B75, B50, B25, and D100 were 68.74, 68.74, 67.52, and 67.49 %, respectively [29].

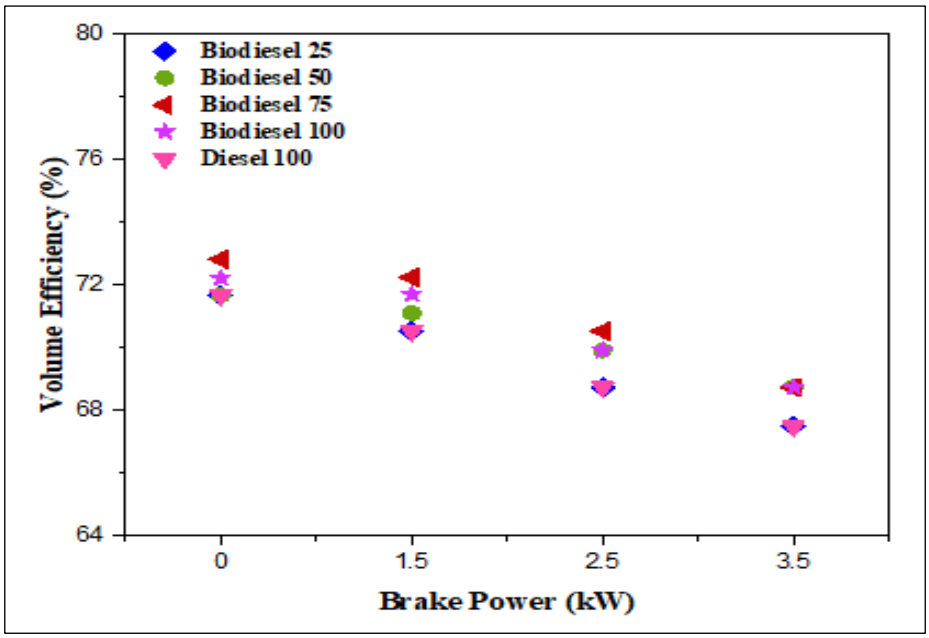

Figure 6: Comparison of VE with engine load for various composition of diesel.
Source: Authors, (2026).

Figure 7 shows the CO_2 emissions associated with the engine's braking power for three different samples: one of biodiesel, one of blended biodiesel, and one of petrodiesel. Biodiesel, blended biodiesel, and petrodiesel exhibited little CO_2 emissions when operating at low engine loads; however, their increased volumetric fuel consumption under high engie loads resulted in elevated CO_2 emissions. Since biodiesel possesses a greater molecular oxygen content and a higher cetane number than petrodiesel, augmenting the petrodiesel content in each sample results in an equivalent rise in the quantity of CO2 present in the exhaust gas. . At full load, B100, B75, B50, and B25 produced CO_2 emissions of 3.81, 3.64, 4.40, 4.72, and 4.17%, respectively.

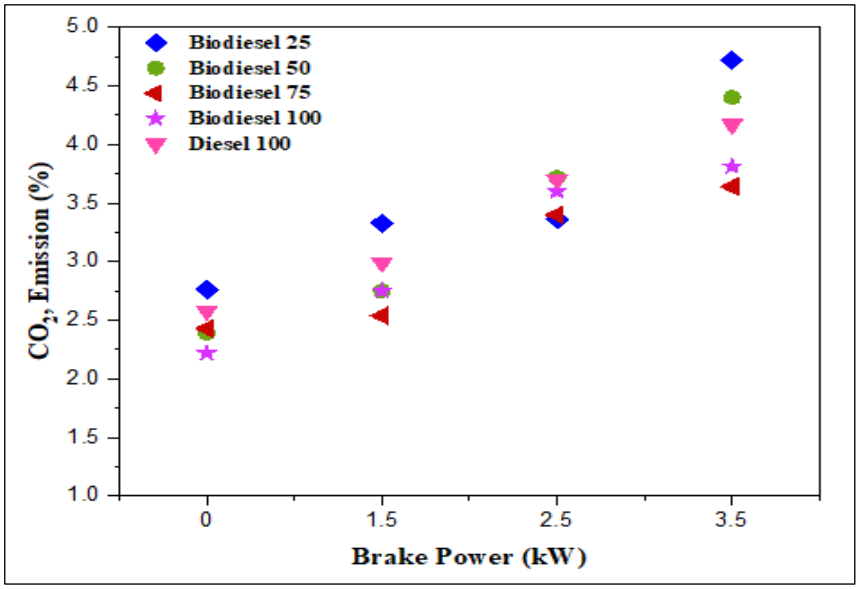

Figure 7: Comparison of CO2 emission with engine load for various samples.
Source: Authors, (2026).

Figure 8 illustrates the carbon monoxide (CO) emission levels from the blended biodiesel samples, petrodiesel, and the biodiesel sample, in conjunction with the associated engine braking power. Minimal engine loads resulted in low CO emissions from biodiesel, blended biodiesel, and petrodiesel. However, high engine loads led to an increase in CO emissions due to factors such as knocking, higher volumetric fuel consumption, and engine power output. Incomplete fuel combustion, together with the fuel's physical and chemical qualities, is the primary determinant of CO emission production. Since petrodiesel has a lower cetane number and a more oxygen-rich molecular structure than biodiesel, increasing the amount of petrodiesel in each sample results in a greater concentration of CO in the exhaust gas. At part load, CO emissions drop as engine load increases for all fuels tested; however, at full load, they rise again as a result of increased fuel consumption. At maximum load operation, the CO emission values for B100, B75, B50, B25, and D100 were 0.075, 0.073, 0.085, 0.088, and 0.091 %, respectively [30].

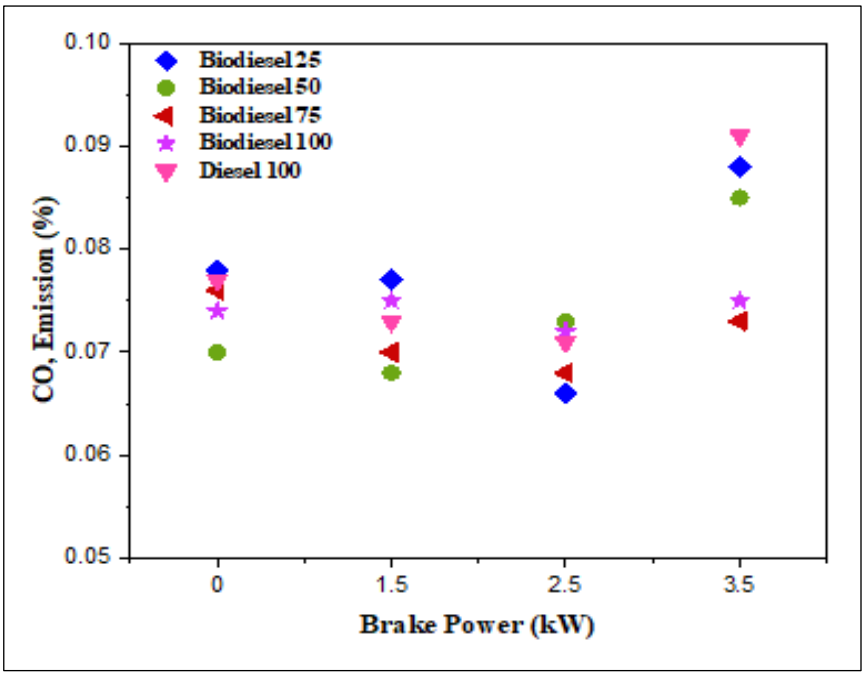

Figure 8: Evaluation of CO emission with engine load for Various composition.
Source: Authors, (2026).

he relationship between oxygen levels and engine braking force is illustrated in Figure 9 for biodiesel, blended biodiesel, and petrodiesel samples. Due to the combustion of a more concentrated mixture within the engine cylinder, the levels of oxygen were significantly elevated during periods of low engine load and diminished during periods of high engine load. Increased petrodiesel concentration in each sample resulted in a reduction in the oxygen content of exhaust gas. This was due to the higher oxygen concentration of biodiesel within its molecular structure in comparison to petrodiesel. At full load, the oxygen concentration values for B100, B75, B50, B25, and D100 were 23.69%, 22.96%, 21.96%, and 23.16%, respectively.

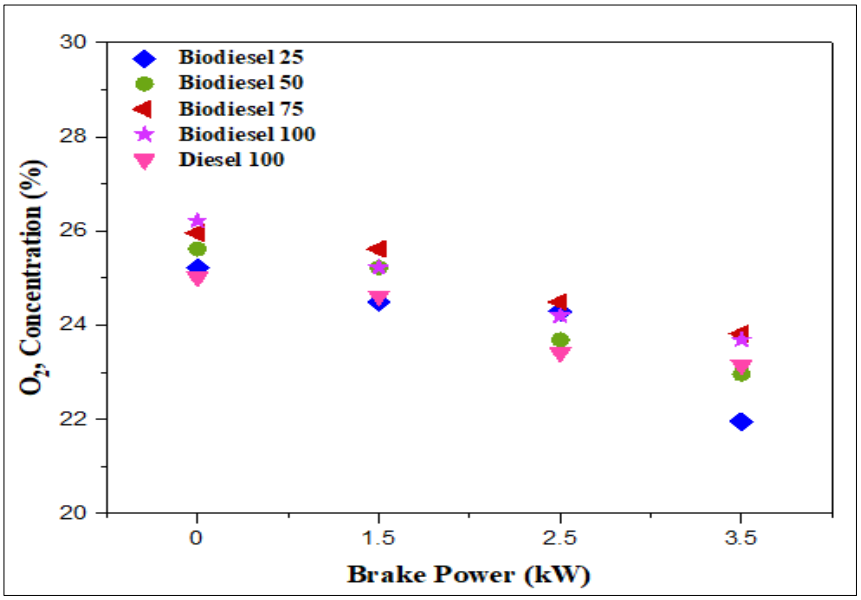

Figure 9: Evaluation of oxygen with engine load for various mixture of biodiesel.
Source: Authors, (2026).

Regarding the engine's braking force, Figure 10 illustrates the HC emission levels of petrodiesel, mixed biodiesel, and biodiesel samples. Hydrocarbon emissions from petrodiesel, mixed biodiesel, and biodiesel were negligible at low engine loads; however, they escalated significantly at high loads as a result of higher fuel injection, which led to less oxygen and greater particle size. In addition to the reduced quantity of Petro diesel present in each sample, the increased concentrations of HC in exhaust gas can be attributed to the higher viscosity, inadequate atomization, and improper fuel-air mixing of biodiesel in comparison to petro-diesel. The HC emission values for B100, B75, B50, B25, and D100, respectively, are 16.77, 15.78, 14.75, 15.74, and 11.70 ppm when operating at full load.

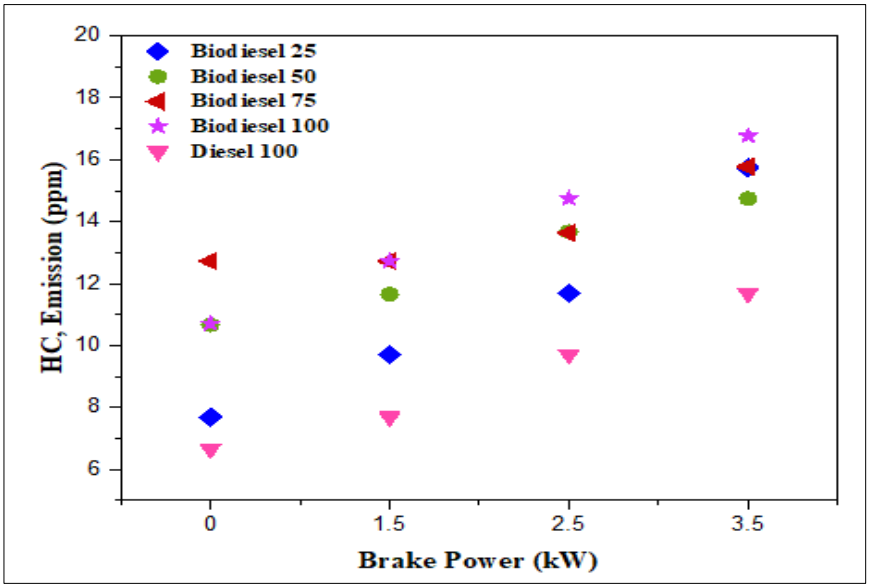

Figure 10: Comparison of hydrocarbon emission with engine load for various mixture of diesel.
Source: Authors, (2026).

IV. CONCLUSION

One of the best green energy options is biodiesel. Some of its many benefits include being very lubricating, having minimal toxicity, not emitting sulphur, and not releasing particle matter pollution. The most popular biodiesel manufacturing process is transesterification because it is easy to use, efficient, has a high conversion rate, and improves the fuel characteristics while reducing the oil's viscosity. In comparison to other catalyst types, NaOH allowed for a larger ester content, was inexpensive, and had a number of other desirable properties, making it an ideal as an alkaline homogeneous catalyst. As a result of its inexpensive price, low density, molecular weight, and viscosity —all of which facilitate rapid solubility and diffusion—C2H6O was considered the optimal alcohol for implementation in the transesterification process. The results were assessed using a S of 9:1, a T of 30°C, and a t of 80 minutes. The anticipated maximum biodiesel recovery was 98.22%. Five runs were performed with the settings indicated above, resulting in an average biodiesel recovery percentage of 96.68 % with a standard deviation of 0.48. With an error rate of less than 2.6%, the proposed model is clearly valid. The production of methyl ester of the majority of triglycerides was confirmed by GC-mass and FTIR.

The created biodiesel was determined to be comparable to commercial biodiesel and its blends derived from CO, as well as pure petrodiesel and biodiesel blends, following diesel engine testing (B75, B50, and B25). The findings indicated that the biodiesel exhibited superior efficiency and reduced emissions in comparison to the petrodiesel. In comparison to petrodiesel, the volumetric efficiency, SFC, TE, EGT, and emissions concentrations of Carbon monoxide, Carbon dioxide, and Oxygen were all enhanced by the CO biodiesel and its mixes.

V. AUTHOR'S CONTRIBUTION

Conceptualization: Sangeetha Krishnamoorthi.
Methodology: Prabhu L, Saravanan M.
Investigation: Saravanan M, Mahesh R.
Discussion of results: Sangeetha Krishnamoorthi, Prabhu L
Writing – Original Draft: Sangeetha Krishnamoorthi.
Writing – Review and Editing: Hariharan, Venukumar.
Resources: Sangeetha Krishnamoorthi.
Supervision: Prabhu L.
Approval of the final text: Sangeetha Krishnamoorthi, Prabhu L, Mahesh R.

VI. REFERENCES

[1] E. J. Mendes de Paiva, J. C. S. Barboza, M. L. C. P. da Silva, H. F. de Castro, and D. S. Giordani, "Comparative study of biodiesel production from ethanol and babassu oil using mechanical agitation and ultrasounds," Renewable Energy and Power Quality Journal, vol. 1, no. 9, pp. 1250–1253, 2011

[2] Patra, C. J., Kumaran, P., Praveen, R., & Kumar, A. S. Production of biodiesel from spent coffee grounds by transertification and its byproducts as fuel additives. Int. J. Chem. Sci, 14, 590-596, 2016.

[3] H. Li, Q.-S. Zhao, S.-L. Chang, T.-R. Chang, M.-H. Tan, and B. Zhao, "Development of cannabidiol full-spectrum oil/2,6-di-O-methyl-β-cyclodextrin inclusion complex with enhanced water solubility, bioactivity, and thermal stability," J Mol Liq, vol. 347, 2022

[4] J. M. Priebe, E. L. Dall'Oglio, P. T. De Sousa, L. G. De Vasconcelos, and C. A. Kuhnen, "Measurement of Physicochemical Properties during Microwave-Assisted Acid-Catalyzed Transesterification Reactions," Energy and Fuels, vol. 30, no. 4, pp. 3066–3077, 2016

[5] D. Chesterfield, P. L. Rogers, E. Al-Zaini, and A. A. Adesina, "Steady-state simulation of a novel extractive reactor for enzymatic biodiesel production," in Fuel Processing Technology, 2013, pp. 101–111.

[6] H. Nayebzadeh, N. Saghatoleslami, and M. Tabasizadeh, "Optimization of the activity of KOH/calcium aluminate nanocatalyst for biodiesel production using response surface methodology," J Taiwan Inst Chem Eng, vol. 68, pp. 379–386, 2016

[7] B. Maleki and S. S. Ashraf Talesh, "Pour point and yield simultaneous improvement of alkyl esters produced by ultrasound-assisted in the presence of αFe2O3/ZnO: RSM approach," Fuel, vol. 298, 2021

[8] A. K. R. Somidi, U. Das, and A. K. Dalai, "One-pot synthesis of canola oil based biolubricants catalyzed by MoO3/Al2O3 and process optimization study," Chemical Engineering Journal, vol. 293, pp. 259–272, 2016

[9] M. A. Hazrat et al., "Biodiesel production from transesterification of Australian Brassica napus L. oil: optimisation and reaction kinetic model development," Environ Dev Sustain, vol. 25, no. 11, pp. 12247–12272, 2023

[10] Y. Kassem, H. Gökçekuş, and H. Çamur, "Prediction of kinematic viscosity and density of biodiesel produced from waste sunflower and canola oils using ann and rsm: Comparative study," in Advances in Intelligent Systems and Computing, 2020, pp. 880–887.

[11] B. Maleki and S. S. A. Talesh, "Optimization of the Sono-Biodiesel in the Attendance of ZnO Nanoparticles, Process Yield Enhancement: Box Behnken Design," Journal of Chemical and Petroleum Engineering, vol. 56, no. 1, pp. 1–14, 2022, [Online]. Available: https://www.scopus.com/inward/record.uri?eid=2-s2.0-85132004011&doi=10.22059%2fJCHPE.2021.330251.1361&partnerID=40&md5=52ef70b767f1420615b619de54b8aac8

[12] A. Ghalandari, M. Taghizadeh, and M. Rahmani, "Statistical Optimization of the Biodiesel Production Process Using a Magnetic Core-Mesoporous Shell KOH/Fe3O4@γ-Al2O3 Nanocatalyst," Chem Eng Technol, vol. 42, no. 1, pp. 89–99, 2019

[13] X. Zhang, N. T. Lan Chi, C. Xia, A. S. Khalifa, and K. Brindhadevi, "Role of soluble nano-catalyst and blends for improved combustion performance and reduced greenhouse gas emissions in internal combustion engines," Fuel, vol. 312, 2022

[14] C. Enweremadu, O. Samuel, and H. Rutto, "Experimental Studies and Theoretical Modelling of Diesel Engine Running on Biodiesels from South African Sunflower and Canola Oils," Environmental and Climate Technologies, vol. 26, no. 1, pp. 630–647, 2022

[15] M. Omraei, S. Sheibani, S. M. Sadrameli, and J. Towfighi, "Preparation of biodiesel using KOH-MWCNT catalysts: An optimization study," Ind Eng Chem Res, vol. 52, no. 5, pp. 1829–1835, 2013

[16] B. Maleki and S. S. Ashraf Talesh, "Optimization of ZnO incorporation to αFe2O3 nanoparticles as an efficient catalyst for biodiesel production in a sonoreactor: Application on the CI engine," Renew Energy, vol. 182, pp. 43–59, 2022

[17] M. Opuz, A. Uyumaz, M. Babagiray, H. Solmaz, A. Calam, and F. Aksoy, "The effects of metallic fuel addition into canola oil biodiesel on combustion, engine performance and exhaust emissions," Journal of the Energy Institute, vol. 111, 2023

[18] M. R. Afshar Mogaddam, M. A. Farajzadeh, S. Azadmard Damirchi, and M. Nemati, "Dispersive solid phase extraction combined with solidification of floating organic drop–liquid–liquid microextraction using in situ formation of deep eutectic solvent for extraction of phytosterols from edible oil samples," J Chromatogr A, vol. 1630, 2020

[19] Ü. Ağbulut, “Understanding the role of nanoparticle size on energy, exergy, thermoeconomic, exergoeconomic, and sustainability analyses of an IC engine: A thermodynamic approach,” Fuel Processing Technology, vol. 225, 2022

[20] K. Muric, P. Tunestal, A. Andersson, and L. Andersson, “Thermal Reduction of NOx in a Double Compression Expansion Engine by Injection of AAS 25 and AUS 32 in the Exhaust Gases,” in SAE Technical Papers, 2019.

[21] A. K. R. Somidi, P. K. Roayapalley, and A. K. Dalai, “Synthesis of O-propylated canola oil derivatives using Al-SBA-15 (10) catalyst and study on their application as fuel additive,” Catal Today, vol. 291, pp. 204–212, 2017

[22] M. Lee et al., “Optimization of enzymatic biodiesel synthesis using RSM in high pressure carbon dioxide and its scale up,” Bioprocess Biosyst Eng, vol. 36, no. 6, pp. 775–780, 2013

[23] T. Marshall and E. Pensini, “Vitamin B12 and Magnesium: a Healthy Combo for the Degradation of Trichloroethylene,” Water Air Soil Pollut, vol. 232, no. 8, 2021

[24] Kumaran, P., S. Natarajan, R. Shanmuga Raj, S. Dhanaraj, and V. Rubesh Kumar. "Performance and emissions on VCR diesel engine with turbocharger setup running using tomato seed oil." Materials Today: Proceedings 45, 6078-6082, 2021.

[25] A. Athimoolam and S. Ramakrishnapillai, “Performance, combustion, and emission characteristics of direct injection diesel engine fueled with ZnO dispersed canola oil biodiesel,” Advances in Environmental Technology, vol. 8, no. 2, pp. 159–168, 2022

[26] P. K. Hari, S. C. Ananda, and K. K. Praveen, “Performance and emission evaluation of direct inejction diesel engine using canola, sesame biodiesels with n-butanol,” Strojnicky Casopis, vol. 71, no. 1, pp. 139–148, 2021

[27] Kumaran, P., Natarajan Sengodan, Sudesh Kumar MP, A. Anderson, and S. Prakash. "Investigating the emissions and performance of ethanol and biodiesel blends on Al2O3 thermal barrier coated piston engine using response surface methodology design-multiparametric optimization." Environmental Research and Technology 7, no. 3 (2024): 406-421.

[28] L. Wißmann, S. Crönert, S. Welscher, M. Grill, and M. Bargende, “Detailed Numerical Investigation of the Influences of External Water, Lubricating Oil and Reactive EGR Components on ICE Ignition Processes,” in COMODIA 2022 - 10th International Conference on Modeling and Diagnostics for Advanced Engine Systems, 2022, pp. 44–53.

[29] M. G. Jang, D. K. Kim, S. C. Park, J. S. Lee, and S. W. Kim, “Biodiesel production from crude canola oil by two-step enzymatic processes,” Renew Energy, vol. 42, pp. 99–104, 2012

[30] F. Esmi, A. K. Dalai, and Y. Hu, “Optimization and kinetic studies of 12-tungstophosphoric supported mesoporous aluminosilicate through response surface methodology for biodiesel production using green seed canola oil,” Fuel, vol. 348, 2023.